

## THE TRANSFORMATION OF LEPIDOCROCITE DURING HEATING: A MAGNETIC AND SPECTROSCOPIC STUDY

A. U. GEHRING<sup>1</sup> AND A. M. HOFMEISTER<sup>2</sup>

<sup>1</sup> Department of Soil Science, University of California,  
Berkeley, California 94720

<sup>2</sup> Department of Geology, University of California,  
Davis, California 95616

**Abstract**—Infrared (IR) spectroscopy, in combination with magnetic methods, was used to study the thermally induced transformation of synthetic lepidocrocite ( $\gamma$ -FeOOH) to maghemite ( $\gamma$ -Fe<sub>2</sub>O<sub>3</sub>). Magnetic analyses showed that the thermal conversion began at about 175°C with the formation of superparamagnetic maghemite clusters. The overall structural transformation to ferrimagnetic  $\gamma$ -Fe<sub>2</sub>O<sub>3</sub> occurred at 200°C and was complete around 300°C. At higher temperatures, the maghemite converted into hematite ( $\alpha$ -Fe<sub>2</sub>O<sub>3</sub>). Observation of the transformation from  $\gamma$ -FeOOH to  $\gamma$ -Fe<sub>2</sub>O<sub>3</sub> using variable-temperature IR spectroscopy indicated that dehydroxilation on a molecular level was initiated between 145°C and 155°C. The lag time between the onset of the breaking of OH bonds and the release of H<sub>2</sub>O from lepidocrocite around 175°C can be explained by diffusive processes. Overall dehydroxilation and the subsequent breakdown of the lepidocrocite structure was complete below 219°C. The comparison of the magnetic and IR data provides evidence that the dehydroxilation may precede the structural conversion to maghemite.

**Key Words**—Dehydroxilation, IR spectra, Lepidocrocite, Maghemite, Phase transformation.

### INTRODUCTION

Lepidocrocite ( $\gamma$ -FeOOH) is well known to occur in pedogenic environments particularly in humid and temperate regions (Schwertmann, 1989). Under ambient conditions, lepidocrocite can be transformed to its polymorph goethite ( $\alpha$ -FeOOH) (e.g., Schwertmann and Taylor, 1972). Upon heating to approximately 250°C, lepidocrocite converts to maghemite ( $\gamma$ -Fe<sub>2</sub>O<sub>3</sub>). This conversion, e.g., during forest and bush burning, has been considered a major maghemite forming process in tropical and subtropical soils (Schwertmann, 1989).

The transformation from  $\gamma$ -FeOOH to  $\gamma$ -Fe<sub>2</sub>O<sub>3</sub>, characterized by a well-defined loss of structural water and a change from a paramagnetic to a ferrimagnetic phase, has been studied in detail (Subrt *et al.*, 1981; Gómez-Villacieros *et al.*, 1984; Morris *et al.*, 1985). In a recent study, Gehring *et al.* (1990) described an activated state on the molecular level within the lepidocrocite structure prior to the actual evolution of water and the subsequent formation of ferrimagnetic maghemite. This state has been explained as an enhanced distortion of FeO<sub>6</sub> octahedra in the lepidocrocite structure caused by the dynamic rearrangement of the position of oxygen and hydrogen atoms. The relation between the activated state and the dehydroxilation of the lepidocrocite structure on a molecular level has not been studied thus far. Infrared (IR) spectroscopy is a powerful tool for monitoring dehydroxilation

in minerals on a molecular level (Farmer, 1974) and, therefore, opens the door to provide additional information about the transformation from  $\gamma$ -FeOOH to  $\gamma$ -Fe<sub>2</sub>O<sub>3</sub>.

In this investigation, IR spectroscopy is used in combination with magnetic methods to analyze the structural changes of lepidocrocite during the conversion to maghemite.

### EXPERIMENTAL PROCEDURES

Lepidocrocite was prepared by oxidation of a 0.5 M FeCl<sub>2</sub> solution with NaNO<sub>2</sub> after the method described by Glemser (1938). The synthetic lepidocrocite was identified by X-ray powder diffractometry with a Guinier IV camera (model TR552, Enraf Nonius) using Cu-K $\alpha$  radiation. The bulk susceptibility of untreated and stepwise heated samples was measured on a KLY-2 Susceptibility Bridge with a sensitivity of  $4 \times 10^{-8}$  [SI]. Thermomagnetic analysis was performed on powder samples in a 0.2 mT field, using a horizontal motion Curie balance (Lebel, 1985) in order to trace the creation of, or the change in, the ferromagnetic mineralogy during heating.

Electron paramagnetic resonance (EPR) spectra were recorded on a Bruker 200ER spectrometer, operating at X-band frequency with 100 kHz field modulation. The spectrometer settings were 2 mW microwave power, 0.1 mT modulation amplitude, and 9.38 GHz frequency. All spectra were recorded at room temperature (RT) for untreated samples and samples heated stepwise between 100° and 500°C for 0.5 h at 25°C or 50°C steps in an oven. The EPR derivative spectra were processed to determine the *g*-values [N,N-diphenylpi-

<sup>1</sup> Present address: Swiss Federal Institute for Forest, Snow and Landscape Research, 8903 Birmensdorf, Switzerland.

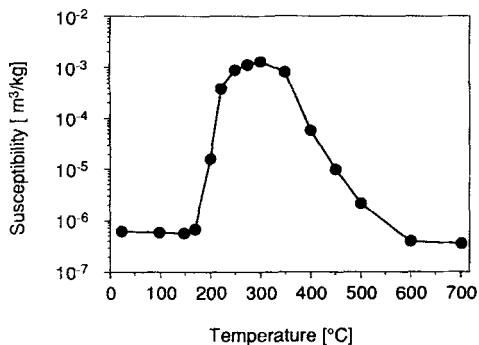


Figure 1. Bulk susceptibility vs. temperature of lepidocrocite powder after stepwise heating in an oven for 0.5 h at each step.

crylhydrazyl (DPPH) as *g*-reference] using computer-scope programs from R. C. Electronics (Santa Barbara, California).

Infrared spectra were obtained from finely ground samples that were dispersed between CsI or KBr windows by rubbing them together. The spectra were collected at various temperatures using a programmable Spectra-Tech heating cell in an evacuated Bomem DA 3.02 Fourier transform interferometer. Samples were heated with a step-gradient starting at RT. Far-IR spectra were obtained over 1 h at each step with 2  $\text{cm}^{-1}$  resolution with a deuterated triglycine sulfate pyroelectric detector and a 3  $\mu\text{m}$  mylar beam splitter. Mid-IR spectra were obtained over 0.5 h at 1  $\text{cm}^{-1}$  resolution with a HgCdTe detector and a KBr beam splitter. Mid-IR spectra were also collected at 176°C as a function of time over 48 h. Baselines were determined using clean windows under the same conditions. Temperatures of the cell were calibrated by inserting a type-S wire thermocouple between the two windows of an empty cell and comparing the thermocouple reading with the nominal temperature displayed on the controller. The calibration was approximately linear, with a controller reading of 400°C corresponding to 344°C in the cell. The calibration curve is unlikely to be affected by addition of very small amounts of lepidocrocite sample.

For comparison, IR spectra of lepidocrocite, goethite, and maghemite were also acquired from powder that was compressed into a thin film of about 1  $\mu\text{m}$  thickness with a megabar diamond anvil cell (DAC). The goethite sample used was previously described (Gehring and Karthein, 1989). Maghemite was produced from lepidocrocite by heating at 250°C in air for about 1 h. As discussed by Hofmeister *et al.* (1992), the thin-film technique is quantitative and yields peak positions close to the transverse optic modes. Type-IIa diamonds were used and the film thicknesses were in the  $\mu\text{m}$  range. Far-IR absorption spectra were collected in 500 scans at 1  $\text{cm}^{-1}$  resolution from  $\sim 100$  to

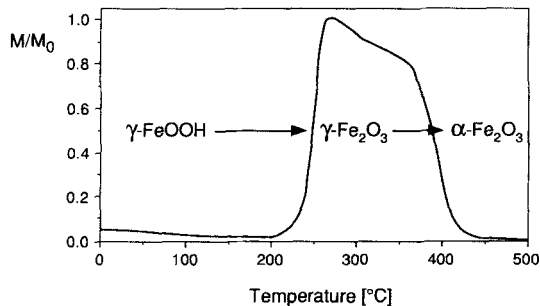


Figure 2. Thermomagnetic curve in an external magnetic field of 0.2 mT of lepidocrocite powder sample.

750  $\text{cm}^{-1}$  with a helium-cooled Si bolometer and a 3  $\mu\text{m}$  mylar beam splitter.

## RESULTS

The X-ray diffraction pattern of the synthetic lepidocrocite powder was consistent with that of single-phase material (JCPDS, 1980). Lepidocrocite has a bulk susceptibility ( $X$ ) of  $61.6 \times 10^{-8} \text{ m}^3/\text{kg}$  (Figure 1). Upon heating,  $X$  remained stable up to 175°C. At higher temperatures, a drastic increase in  $X$  of more than three orders of magnitude was observed. The maximum  $X = 12.6 \times 10^{-4} \text{ m}^3/\text{kg}$  was reached at approximately 300°C (Figure 1). Further heating led to a drop in  $X$ , and values similar to the initial one for lepidocrocite were found above 500°C. Thermomagnetic analysis showed a smooth drop of the magnetization during heating up to 200°C (Figure 2). A steep increase was observed above 200°C, and the maximum magnetization was found at 273°C. The decay of the induced magnetization occurred in two steps, with a pronounced decrease up to 380°C and a further steep drop in magnetization between approximately 380°C and 450°C (Figure 2).

The EPR spectrum of the lepidocrocite exhibited a broad signal near  $g = 2$ . Upon heating of the sample to 175°C, a spectral change was observed. The newly formed signal had a  $g$ -value of 2 and superimposed the broader spectrum of lepidocrocite (Figure 3b). Further heating led to broadening of the  $g = 2$  signal and the formation of an asymmetric signal with  $g \approx 2.5$  and a line-width of 135 mT. This signal reached its maximum intensity at 300°C (Figure 3c). After annealing at higher temperature, a decrease in intensity was observed and, at 500°C, the signal disappeared (Figures 3d and 3e).

Far-IR spectra of lepidocrocite at RT obtained from a thin-film showed three distinct peaks (230, 266, and 356  $\text{cm}^{-1}$ ), and a broad poorly resolved band at 470  $\text{cm}^{-1}$  (Figure 4). Shoulders were found at approximately 300, 320, and 420  $\text{cm}^{-1}$ . Some additional features (e.g., 280  $\text{cm}^{-1}$  and below 200  $\text{cm}^{-1}$ ) were not reproducible and are not further discussed. Many of the peak positions of lepidocrocite (Table 1) resembled

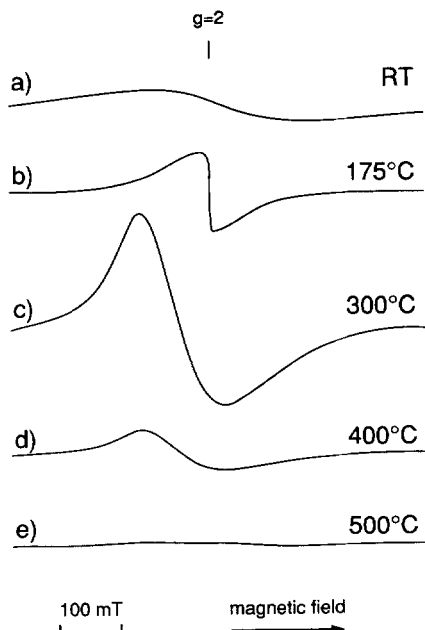


Figure 3. Electron paramagnetic resonance spectra of lepidocrocite at RT, and after stepwise heating to 175°, 300°, 400°, and 500°C.

those of goethite, but the relative intensity patterns of these minerals differed considerably (Figure 4).

The spectra obtained at RT from the heating cell (Figure 5, bottom) and the thin-film were similar regarding the positions and intensities of the well-resolved bands at 263 and 362  $\text{cm}^{-1}$ . By contrast, the position of the peak at the lowest wavenumber differed by 14  $\text{cm}^{-1}$  from that yielded by the thin-film (see Table 1), presumably because of its proximity to the cut-off wavenumber of the CsI windows used. The broad band near 470  $\text{cm}^{-1}$  was even more poorly resolved in the spectrum obtained from the heating cell (Figures 4 and 5). The bands in the range 500–200  $\text{cm}^{-1}$  can be assigned to lattice vibrations. Sharp peaks near 440 and 510  $\text{cm}^{-1}$  in the spectrum at RT disappeared immediately upon heating and were not seen for the thin-film spectra and can, therefore, be considered as artifacts.

In the mid-IR region, lepidocrocite showed sharp peaks at 739, 1015, and 1159  $\text{cm}^{-1}$  that can be assigned to  $\delta$ -OH bending bands (Lewis and Farmer, 1986). A decrease in transmission observed towards high wavenumbers (<1100  $\text{cm}^{-1}$ ) is probably from scattering by exsolved water within the heating cell itself because the KBr windows became increasingly cloudy with use.

Maghemite, formed via heating of lepidocrocite at 250°C for 1 h in an oven, exhibited four bands in the far-IR region (Figure 4, Table 1). The bands (319, 399, 449, and 571  $\text{cm}^{-1}$ ) were poorly resolved due to large breadth and low intensity (Figure 4). The positions

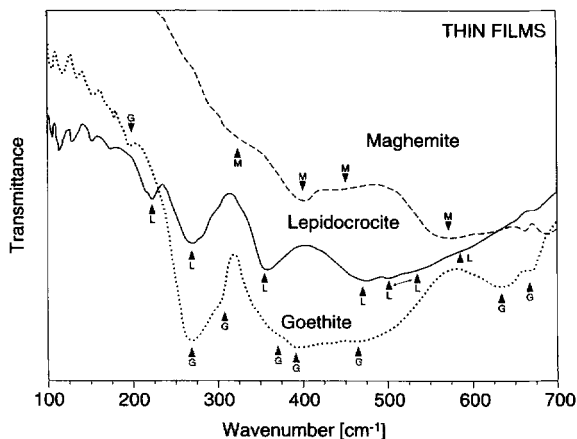


Figure 4. Far-IR spectra of iron hydroxides and oxides at RT obtained from thin-films in the diamond anvil cell. The peaks and shoulders were confirmed to be intrinsic by taking spectra at various sample thicknesses. Noise below and above 600  $\text{cm}^{-1}$  was reduced by smoothing.

coincided with those from four of the six IR modes of hematite (Serna et al., 1982). The  $\gamma$ - $\text{Fe}_2\text{O}_3$  spectrum resembled those of other spinels with a high charge cation in the octahedral site (e.g.,  $\text{FeAl}_2\text{O}_4$ ; Chopelas and Hofmeister, 1991). Accordingly, the four bands can be assigned to translation of  $\text{Fe}^{3+}$  in the tetrahedral site (319  $\text{cm}^{-1}$ ), to a bend of the  $\text{FeO}_6$  octahedra (399

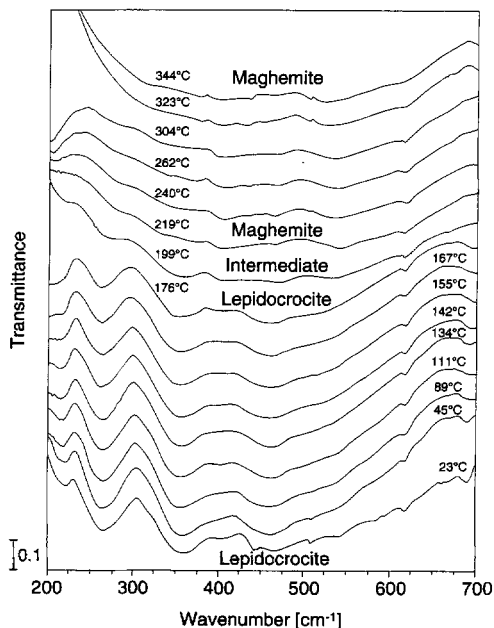


Figure 5. Far-IR spectra of lepidocrocite acquired from a heating cell with a step-gradient starting at RT. The spectra are offset sequentially by 0.05 transmittance units. Scale bar indicates 0.1 transmittance unit.

Table 1. Infrared wavenumbers of iron hydroxides and oxides and their dependencies on temperature.

	Temperature °C	Far-IR						Mid-IR							
$\alpha$ -FeOOH	RT, thin film	196	267	302	365	391	474			635	667	794	898		
$\gamma$ -FeOOH	RT, thin film	230	266		356		470	500–535	580			742 <sup>1</sup>		1018 <sup>1</sup>	1160 <sup>1</sup>
$\gamma$ -FeOOH	RT, heated cell	216	263		362	~405	470	540	582			739	904	1015	1159
	45	217	263		356	~405	470	542	589			738.9	~891	1013.5	1151
	89	217	263		355	~405	466	542	590			734.7	~893	1009	1157
	111	217	263		355	~405	466	542	595			732.5	~896	1007.3	1151
	124	217	263		352	~405	466	542				730.4	~890	1007	1142
	142	217	263		355		462	542				730	~885	1004.8	1140
	155	217	263		355		462	542				726.7		1004.6	
	167	?	263		355		462	542				726.7		1004.6	
	176	?	263		355		462					720.4		1004.6	
Intermediate	199	217			350–362	405	470	540				nm	nm	nm	nm
$\gamma$ -Fe <sub>2</sub> O <sub>3</sub>	219		275?			405		540				718 sh			
	240		275?			405	~470	540	630 sh			718 sh			
	262		275?			405	~470	540				710 sh			
	284		nm			nm		nm	630sh			710sh			
	304		275?			405	~470	540				708sh			
	323			320?		400		533				nm			
	344							533				615 sh		716 sh	
	23											627		728 sh	
	133											615		721 sh	
	262											623		719 sh	
	384											629		708 sh	
$\gamma$ -Fe <sub>2</sub> O <sub>3</sub>	RT, thin film			319		399		449 571							
$\alpha$ -Fe <sub>2</sub> O <sub>3</sub> <sup>2</sup>	RT, thin film	229		300–335		380–400		440–470 525–540		625–650					

<sup>1</sup> Frequencies from KI pellets as compiled by Lewis and Farmer (1986).

<sup>2</sup> Data from Serna *et al.*, 1982. Peak positions depend on particle shapes as indicated by the ranges given. sd = shoulder, nm = not measured.

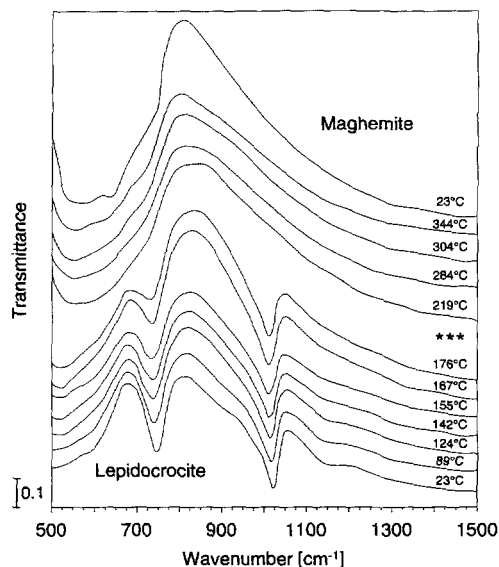


Figure 6. Mid-IR spectra of lepidocrocite acquired from a heating cell with a step-gradient starting at RT. Asterisks mark the transformation temperature range. In the two groups of spectra separated by asterisks, single spectra are offset by 0.05 transmittance units. Scale bar indicates 0.1 transmittance unit.

$\text{cm}^{-1}$ ), to a deformation of the octahedra ( $449 \text{ cm}^{-1}$ ), and to the  $\text{Fe}^{3+}\text{-O}$  stretching motion of the octahedra ( $571 \text{ cm}^{-1}$ ), respectively. These assignments are compatible with symmetry analysis of the spinel structure, but they can only be confirmed by further investigations on single-crystal IR spectra of iron-bearing spinels. Peak positions for maghemite do not precisely match earlier data (McDevitt and Baun, 1964). Problems frequently encountered in obtaining reliable spectra from powder dispersions (Hofmeister, 1991) are magnified for maghemite because it contains only broad, poorly resolved peaks.

Infrared spectra in the  $200\text{--}700 \text{ cm}^{-1}$  range of the lepidocrocite in the heating cell exhibited no significant changes upon heating to  $176^\circ\text{C}$  (Figure 5, lower half). At  $199^\circ\text{C}$ , the spectrum flattened out and peaks at 230, 266, and  $356 \text{ cm}^{-1}$  were retained, but were lower in intensity. In addition, a broad peak occurred at about  $540 \text{ cm}^{-1}$ . At the next temperature measured,  $219^\circ\text{C}$ , the well-resolved, low wavenumber peaks of  $\gamma\text{-FeOOH}$  were no longer discernible. Poorly resolved features found near 400 and  $540 \text{ cm}^{-1}$  for temperatures above  $199^\circ\text{C}$  occurred near the positions of the most intense peaks of the maghemite ( $399$  and  $571 \text{ cm}^{-1}$ ) obtained from thin-film (Figure 4). Shoulders that were present near 300 and  $450 \text{ cm}^{-1}$  (Figure 4 and 5) probably correspond to the remaining two lattice modes of  $\gamma\text{-Fe}_2\text{O}_3$ . Additional peaks (Figure 5) were most likely artifacts induced by scattering from irregular surface and may explain previous difficulties in obtaining a consistent reliable spectrum for maghemite from powder disper-

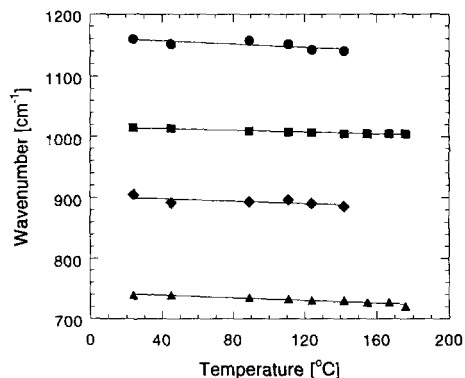


Figure 7. Dependence of mid-IR peaks of  $\gamma\text{-FeOOH}$  on temperature. All of these modes are associated with motions of OH. The lines are least-squares fits to the data.

sion (Farmer, 1974). Scattering alters the relative contribution of the transverse optic (TO) and longitudinal optic (LO) components to the IR peaks in a powder spectrum and also introduces surface modes. If LO components lie at much higher frequencies than the TO mode (ca.  $100 \text{ cm}^{-1}$  difference), then scattering can also produce additional peaks at the LO frequencies (see Serna *et al.*, 1982; McMillan and Hofmeister, 1988, and references therein).

The mid-IR spectrum of  $\gamma\text{-FeOOH}$  was virtually unchanged as temperature was increased to  $145^\circ\text{C}$  (Figure 6, lower half). Between  $142^\circ\text{C}$  and  $155^\circ\text{C}$ , the peaks ( $739$ ,  $1015$ ,  $1159 \text{ cm}^{-1}$ ) associated with motions of OH decreased slightly in intensity. The decrease was more pronounced upon heating to  $176^\circ\text{C}$ . At the next temperature measured,  $219^\circ\text{C}$ , no peaks associated with hydrogen in  $\gamma\text{-FeOOH}$  were observed. Only the highest wavenumber  $\text{Fe}^{3+}\text{-O}$  stretching band ( $\approx 718 \text{ cm}^{-1}$ ) of  $\gamma\text{-Fe}_2\text{O}_3$  was found and no changes were observed up to the highest temperature measured. After cooling the sample to RT, the spectrum was similar, with well-resolved shoulders at 627 and  $728 \text{ cm}^{-1}$ . These shoulders were probably LO or surface modes, exaggerated in intensity because of the irregular sample thickness.

Infrared spectra obtained at  $176^\circ\text{C}$  as a function of time showed that dehydroxilation progressed to completion over 48 h indicated by gradual loss of  $\delta\text{-OH}$  bands. The change between 0.5 and 1 h, the time range of the spectroscopic experiments, was not significant.

Frequencies of the lattice modes of both  $\gamma\text{-FeOOH}$  and  $\gamma\text{-Fe}_2\text{O}_3$  were essentially independent of temperature. The  $474 \text{ cm}^{-1}$  band of lepidocrocite may decrease in intensity with increasing temperature, but the position of this band was uncertain due to its breadth (Table 1). In contrast, the peaks associated with motions of OH ( $700\text{--}1200 \text{ cm}^{-1}$ ) in lepidocrocite decreased definitely and linearly with temperature (Figure 7). Since for other types of bending modes changes with compression have been shown (Chopelas and Hof-

meister, 1991), the 1% to 2% decrease in wavenumber (Table 1) could be assigned to expansion of the lattice. This, however, would suggest an extremely large thermal expansivity,  $60 \times 10^{-6}/\text{K}$ , assuming that wavenumber is proportional to volume. Thus, the change in wavenumber must also reflect a decrease in bonding strength as temperature increases. This inference is supported by the decrease of the OH stretching frequency as hydrogen bonding increases as shown by Nakamoto *et al.* (1955).

## DISCUSSION

The increase of bulk susceptibility and magnetization vs. temperature shows that maghemite is generated at the expense of lepidocrocite near 200°C. The conversion to ferrimagnetic maghemite is complete at approximately 300°C, as indicated by the maximum in bulk susceptibility and in magnetization (Figure 1 and 2). These results are in good agreement with calorimetric data that showed an endothermic enthalpy change during the transformation of lepidocrocite to maghemite at similar temperatures (Hedley, 1968; Gómez-Villacieros *et al.*, 1984). The decay of magnetization above 300°C can be explained by the generation of hematite that carries a weak antiferromagnetism.

The overall conversion of lepidocrocite to maghemite and hematite can be monitored by EPR. The broad signal near  $g = 2$  for lepidocrocite is characteristic of paramagnetic samples and is mainly caused by dipole-dipole interaction between Fe(III) ions. The drastic increase of the EPR absorption during the development of the asymmetric  $g \approx 2.5$  signal indicates a ferromagnetic resonance and can be explained by the formation of maghemite. Since purely antiferromagnetic crystals should not produce resonance (Martin, 1967), the disappearance of the EPR signal at 500°C indicates a complete structural conversion of maghemite to hematite. In addition to the overall reaction, the newly formed  $g = 2$  signal at 175°C points to structural changes within the lepidocrocite (Figure 3b). This signal can be explained by the formation of a fine-grained, superparamagnetic maghemite precursor since it was not stable on heating to 200°C, the temperature where ferrimagnetic maghemite was generated (Figures 1 and 2).

The IR spectra show that OH removal in lepidocrocite begins at 145° to 155°C, whereas changes in the lattice modes are not discerned below 199°C. Hence, loss of water begins prior to the formation of maghemite, which indicates the actual dehydroxylation of the lepidocrocite structure. The difference between the temperatures at which OH is removed from the structure as shown by IR spectroscopy and the formation of maghemite is most likely connected with the time needed for OH and H to combine to form H<sub>2</sub>O, and its subsequent diffusion.

The slight changes in the  $\delta$ -OH modes detected prior to the overall conversion of the lepidocrocite can be explained by dehydroxylation on a molecular level that can lead to the formation of superparamagnetic maghemite clusters in the lepidocrocite structure as indicated by EPR. Gehring *et al.* (1990) pointed out that the formation of maghemite clusters occurs simultaneously with an enhanced structural distortion of FeO<sub>6</sub> octahedra. This state, defined as an activated state in the lepidocrocite structure (Gehring *et al.*, 1990), occurs in the same temperature range where the changes in  $\delta$ -OH modes were detected. Therefore, it is very likely that this activated state is created through weakening of Fe-OH and O-H bonds.

At 199°C, the far-IR spectrum is intermediate to those of  $\gamma$ -FeOOH and  $\gamma$ -Fe<sub>2</sub>O<sub>3</sub>. It seems most likely that this results from the sample simply being a mixture of the two phases. Vestiges of the lepidocrocite structure may remain until 240°C, as indicated by the shoulders near 300 cm<sup>-1</sup>; however, no OH remains above 219°C. This result is in agreement with the temperature range of the maghemite formation and may suggest that dehydroxylation precedes the structural transformation.

## CONCLUSIONS

The combined magnetic and spectroscopic analyses of the conversion of lepidocrocite to maghemite and hematite can be summarized as follows:

- 1) On a molecular level, dehydroxylation of the lepidocrocite began between 145°C and 155°C, and fine-grained, superparamagnetic maghemite clusters were formed around 175°C.
- 2) The overall conversion of  $\gamma$ -FeOOH to  $\gamma$ -Fe<sub>2</sub>O<sub>3</sub> started at about 200°C with the formation of ferrimagnetic maghemite crystals. Lepidocrocite was totally dehydroxylated upon heating to 219°C, and the formation of maghemite was completed around 300°C. At higher temperatures, maghemite was metastable and converted into hematite around 500°C.
- 3) The difference in temperature between the completion of the release of water from lepidocrocite (<219°C) and the formation of maghemite ( $\approx$ 300°C) suggest that the dehydroxylation precedes the structural conversion.

## ACKNOWLEDGMENTS

The authors are grateful to I. V. Fry (U.C.B.) for providing EPR spectra, to T. E. Young (U.C.D.) for acquiring several of the spectra and baselines and for calibrating the heating cell, and to Dr. R. Loeppert for critical review of the manuscript. This project was supported by the Swiss National Science Foundation (A.U.G., grant no. 8220-028438) and by a Fellowship in Science and Engineering from the David and Lucile Packard Foundation (A.M.H.).

## REFERENCES

- Chopelas, A. and Hofmeister, A. M. (1991) Vibrational spectroscopy of aluminate spinels at 1 atm and of  $\text{MgAl}_2\text{O}_4$  to over 200 kbar: *Phys. Chem. Miner.* **18**, 279–293.
- Farmer, V. C. (1974) *The Infrared Spectra of Minerals*: Mineralogical Society, London.
- Gehring, A. U. and Karthein, R. (1989) ESR study of Fe(III) and Cr(III) hydroxides: *Naturwissenschaften* **76**, 172–173.
- Gehring, A. U., Karthein, R., and Reller, A. (1990) Activated state in the lepidocrocite structure during thermal treatment: *Naturwissenschaften* **77**, 177–179.
- Glemser, O. (1938) Über Darstellung und katalytische Wirksamkeit von reinem  $\gamma\text{-FeOOH}$  und daraus gewonnenen  $\gamma\text{-Fe}_2\text{O}_3$ : *Ber. Dtsch. chem. Ges.* **71**, 158–163.
- Gómez-Villacieros, R., Hernán, L., Morales, J., and Tirado, J. L. (1984) Textural evolution of synthetic  $\gamma\text{-FeOOH}$  during thermal treatment by different scanning calorimetry: *J. Coll. Interf. Sci.* **101**, 392–1400.
- Hedley, I. G. (1968) Chemical remanent magnetization of the  $\text{FeOOH}$ ,  $\text{Fe}_2\text{O}_3$  system: *Phys. Earth Planet. Inter.* **1**, 103–121.
- Hofmeister, A. M. (1991) Comment on “Infrared spectroscopy of the polymorphic series (enstatite, ilmenite, and perovskite) of  $\text{MgSiO}_3$ ,  $\text{MgGeO}_3$ , and  $\text{MnGeO}_3$ ,” by M. Madon and G. D. Price: *J. Geophys. Res.* **96**, 21959–21964.
- Hofmeister, A. M., Rose, T. B., Hoering, T. C., and Kushiro, I. (1992) Infrared spectroscopy of natural, synthetic, and  $^{18}\text{O}$  substituted  $\alpha$ -tridymite: Structural implications: *J. Phys. Chem.* **96**, 10213–10218.
- Joint Committee on Powder Diffraction Standards (JCPDS) (1980) *Mineral Powder Diffraction File, Data Book*: JCPDS International Center for Diffraction Data, Swarthmore, Pennsylvania.
- Lebel, P. (1985) Inbetriebnahme und Verwendung einer Curiewaage: Diploma thesis, ETH Zürich, 73 pp.
- Lewis, D. G. and Farmer, V. C. (1986) Infrared absorption of surface hydroxyl groups and lattice vibration in lepidocrocite ( $\gamma\text{-FeOOH}$ ) and boehmite ( $\gamma\text{-AlOOH}$ ): *Clay Miner.* **21**, 93–100.
- Martin D. H. (1967) *Magnetism in Solids*: MIT Press, Cambridge, Mass.
- McDevitt, N. T. and Baun, W. L. (1964) Infrared absorption study of metal oxides in the low frequency region ( $700\text{--}240\text{ cm}^{-1}$ ): *Spectrochim. Acta* **20**, 799–808.
- McMillan, P. F. and Hofmeister, A. M. (1988) Infrared and Raman spectroscopy: in *Spectroscopic Methods in Mineralogy and Geology*, F.C. Hawthorne, ed., *Reviews in Mineralogy* **18**, 99–160.
- Morris, R. V., Lauer, H. V., Lawson, C. A., Gibson, E. K., Nace, G. A., and Stewart, C. (1985) Spectral and other physicochemical properties of submicron powders of hematite ( $\alpha\text{-Fe}_2\text{O}_3$ ), maghemite ( $\gamma\text{-Fe}_2\text{O}_3$ ), goethite ( $\alpha\text{-FeOOH}$ ), and lepidocrocite ( $\gamma\text{-FeOOH}$ ): *J. Geophys. Res.* **90**, 3126–3144.
- Nakamoto, K., Maargoshes, M., and Rundle, R. E. (1955) Stretching frequencies as a function of distances in hydrogen bonds: *J. Am. Chem. Soc.* **77**, 6480–6488.
- Schwertmann, U. (1989) Occurrence and formation of iron oxides in various pedoenvironments: in *Iron in Soils and Clay Minerals*, J. W. Stucki, B. A. Goodman, and U. Schwertmann, eds., Reidel, Dordrecht, 267–308.
- Schwertmann, U. and Taylor, R. M. (1972) The transformation of lepidocrocite to goethite: *Clays & Clay Minerals* **20**, 151–158.
- Serna, C. J., Rendon, J. L., and Iglesias, J. E. (1982) Infrared surface modes in corundum-type microcrystalline oxides: *Spectrochim. Acta* **38**, 797–802.
- Subrt, J., Hanousek, F., Zapletal, V., Lipka, J., and Hucl, M. (1981) Dehydration of synthetic lepidocrocite ( $\gamma\text{-FeOOH}$ ): *J. Thermal. Anal.* **20**, 61–69.

(Received 21 June 1993; accepted 1 March 1994; Ms. 2389)